Assessment of residual stresses in steels and carbide composites by load and depth sensing indentation with spherical indenter

Fjodor Sergejev and Mihhail Petrov

Tallinn University of Technology, Ehitajate tee 5, 19086 Tallinn, Estonia; fjodor.sergejev@ttu.ee

Abstract. Last developments in indentation and computer simulation techniques for the evaluation of mechanical properties (hardness, fracture toughness) of materials are popular because the test conduction is simple. There is no need for precise and expensive specimens of specific geometry, standard tools (indenters) and equipment are used; a lot of measurements can be conducted on relatively small testpieces. Last studies have shown the possibility for the evaluation of the materials residual stresses using a combined indentation–simulation testing technique. The present study is an attempt to measure residual stresses arising in a carbide composite (conventional hard-metal and cermet) using this combined technique. Conventional steels are tested for comparison and validation of the testing technique. An improved simulation algorithm for the assessment of the residual stresses in materials (steels, carbide composites) by load and depth sensing indentation with spherical indenter of specified properties is proposed. The experimental validation of simulations is performed. Spherical indentation results are proved by scanning electron imaging and 3D optical microscopy. The results of the simulations are in a good agreement with experi-mental indentation data. The used method does not require imaging of the indentation impressions and testing of the stress-free specimen for the localized measurement of the residual stresses. It can be used as a reliable express tool for the assessment of the residual stresses with some approxima-tions regarding friction peculiarities of the Hertzian contact between the spherical indenter and specimen surfaces.

Key words: spherical indentation, residual stress, steels, hardmetals.

1. INTRODUCTION

Due to the difference in thermal expansion coefficients of carbide composite phases and manufacturing process peculiarities, the presence of high residual stresses, both tensile and compressive, is a common feature for these materials. Residual stresses heavily influence the reliability of structural components,

especially the fatigue performance. Taking into consideration that carbide composites (hardmetals and cermets) are a preferred material for metal cutting and forming, where long life of the tool is a crucial factor, determination of the residual stresses becomes especially important [1,2].

Steel is a general engineering material and residual stress can be introduced into structural members during machining and joining procedures, for example, welding. The last one especially needs in-situ stress measurements, which can be carried out by indentation tests.

Hardness tests and the development of the theoretical basis of contact mechanics became a powerful tool for the measurement of various properties of materials. Now it becomes possible to control the indentation process with good precision and simultaneously obtain load–penetration data. The last is typically referred to as the load–displacement (P–h) curve for a particular tip–solid system. With reference to general classification, sharp and blunt indenters are in service of instrumented indentation. Sharp Berkovich three-sided pyramid is commonly used in nanoscale indentations due to its small tip roundness, normally about 100 nm. Advantage of sharp Vickers four-sided pyramid is high-load indentations without cracking. Blunt indenters, compared to sharp ones, offer a wider load choice when cracking must be avoided. This is why spherical indentation is the object of the current study.

Previous experiments and theoretical approaches have revealed that the loading part of the load-displacement curve includes both elastic and plastic deformations while the unloading part is mainly elastic. Better results for the unloading part were obtained after several loading-unloading cycles [3].

By associating unloading part of the curve with elastic recovery, it became possible to correlate the unloading data with the Young's modulus of the specimen material. This approach needs that the contact stiffness of the specimen material and the projected contact area are known. The total stiffness depends both on the contact stiffness (contact stiffness of the specimen material) and instrument frame stiffness.

Loading part of the load–displacement data can be employed to deduce the stress–strain information including yield stress. Pile-up or sink-in effects must be considered for better accuracy as the indenter contact area depends on the type of the material's response to the indentation. Pile-up leads to the underestimation of the projected contact area and sink-in makes it overestimated [4]. It is important to notice that pile-up is not restricted to ductile materials. Depending on the ratio of the elastic modulus (E) and hardness (H), E/H, of the specimen material, the pile-up or sink-in can occur. The type of effect, pile-up or sink-in, depends not only on the material's plasticity but on the size and direction of the residual stress state present in the material. According to the *slip line theory*, the mean contact pressure (p_m) can be correlated with the yield stress of the material, and for ferritic materials it gives $p_m \approx 3\sigma_y$, where σ_y is the yield stress (elastic limit). Taking into account almost similar meaning of H and p_m, the ratio E/H can be replaced with E/σ_y. For the determination of the Young's modulus and stress–

strain data it is possible to take sink-in effect into account using the Sneddon's solution, while pile-up effect can be established only by optical, AFM or SEM measuring procedures [5,6]. Residual stress has no effect on hardness and Young's modulus when contact area is accurately measured [7].

It has been proposed to determine the yield stress and elastic limit with methods, based on an inverse analysis instead of analytical solutions [8]. The main and maybe the most unreliable assumption of these methods is the uniqueness of the indentation curve for a particular combination of mechanical properties of the specimen. The idea of the inverse analysis is to fit the experimental curve with that from the "database" with known material properties. "Database" should be obtained before by means of extensive finite element simulation and this procedure is called direct analysis.

In this paper, an attempt to use the combined indentation-simulation procedure for the measurement of the residual stress state in elastic-plastic materials is made. The experimentally obtained load–displacement indentation curves, made with spherical indenters, are used as an etalon for fitting the simulated indentation curves. Along with the inreverse analysis, these results allow to assess the type and roughly the residual stress state of the materials. The implementation of the indentation-simulation procedure for the assessment of the residual stress state for carbide composites is crucial due to the lack of methods for the measurement of residual stresses at the macroscopic level by non-destructive procedures.

2. EXPERIMENTS

2.1. Tested materials

Different types of materials were selected from two main groups of tool materials. In both groups the mechanical properties between materials varied considerably. The steels are selected to have almost the same elastic limit and different mechanical properties (yield stress and tensile strength). The elastic limit varied in the case of carbide composites. The main mechanical properties like hardness and microstructural parameters and the carbide grain size were similar for the studied materials.

2.1.1. Steels

The first group is the steels – a wear-resistant steel (HARDOX 400) and carbon steel C60E. Those commercially available materials were purchased in the form of sheets, then cut to appropriate dimensions 35.0 × 15.0 × 5.0 mm. Specimens were ground and polished on cloth with 3 μm diamond paste to a surface roughness of about $R_a = 0.4$ μm on two sides (measured along 8 mm of the specimen by the Surtronic 3+ apparatus, using CR filter). The chemical composition of tested steels is given in Table 1. The main mechanical properties of the studied steels are shown in Table 2.

Table 1. Composition of the steels, %

Grade	C	Si	Mn	P	S	Cr	Ni	Mo	Al	B
HARDOX 400	0.14	0.70	1.60	0.025	0.010	0.30	0.25	0.25	–	0.004
C60E	0.61	0.03	0.63	0.008	0.004	0.21	0.05	0.01	0.016	–

Table 2. Main mechanical properties of the steels

Grade	Yield stress $R_{p0.2}$, MPa	Tensile strength R_m, MPa	Elongation A_5[1] and A_{80}[2], %	Brinell hardness, HB	Elastic modulus E, GPa	Poisson ratio ν
HARDOX 400	1000	1250	10.0[1]	370–430	210	0.30
C60E	410	542	23.5[2]	164	190	0.27

The microstructural investigations of the steels were not executed as selected grades are widely used and additional information can be found elsewhere. The aim of the current study is to give emphasis to carbide composites. The future investigations are aimed to cover more materials, like high-speed steels [9].

The chemical composition and main mechanical properties of the steel C60E were measured at the Testing Laboratory of the Tallinn University of Technology. The chemical composition and mechanical properties of the steel HARDOX 400 are taken from the producer certificates of the producer SSAB AB.

2.1.2. Carbide composites

The second group of materials are carbide composites. TiC-based cermet with nickel-molybdenum binder (TiC-Ni/Mo), and conventional hardmetal (WC-Co) are tested. The conventional hardmetal is chosen to make reliable comparison with cermet as it is widely used and a lot of comparative data is available.

Along with the chemical composition, the main mechanical properties can be found from Table 3. All materials were produced in Powder Metallurgy Laboratory at Tallinn University of Technology (TUT). The testpieces were produced through conventional press and vacuum sinter powder metallurgy according to ASTM B406. Then the specimens were cut to the dimensions: $35.0 \times 15.0 \times 5.0$ mm.

Table 3. Composition and mechanical properties of tested carbide composites

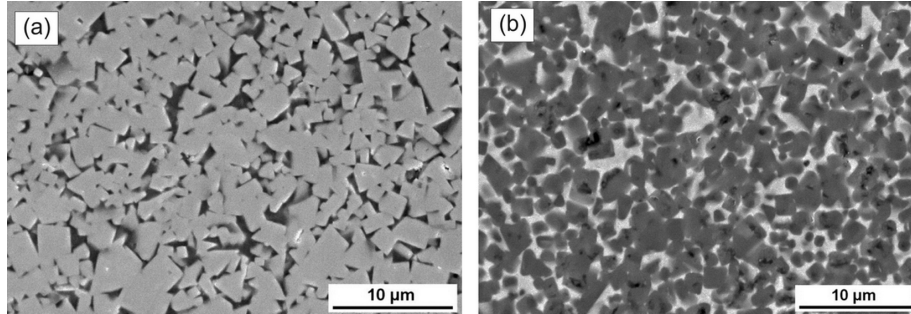| Grade	Composition		Mechanical properties				
	Carbide, wt%	Binder, wt%	Transverse rupture strength R_{TZ}, MPa	Vickers hardness HV, MPa	Elastic modulus E, GPa	Fracture toughness K_{IC}, MPa·m$^{1/2}$	Poisson ratio ν
H15	WC, 85	Co, 15	2900	1170	560	15.2	0.23
T30A	TiC, 70	Ni/Mo, 30	1600	1280	395	16.9	0.31

Fig. 1. SEM micrographs of the tested H15 (a) and T30A (b) carbide composite.

Table 4. Microstructure parameters of studied carbide composites

Grade	Average carbide grain size d_g, μm	Contiguity C	Binder mean free path d_{binder}, μm
H15	1.98	0.50	1.30
T30A	2.00	0.38	1.37

Finally, specimens were ground and then polished using the polishing cloth and 1 μm diamond paste to a surface roughness of about $R_a = 0.2$ μm on two sides (measured along 8 mm of the specimen by the Surtronic 3+ apparatus, using CR filter, see Fig. 1). Opposite ground faces were parallel within 0.03 mm. In order to remove surface contaminants, the samples were cleaned in alcohol and dried by compressed air.

Additional microstructure parameters of studied materials are shown in Table 4. Mean carbide grain size, carbide contiguity C (a measure of the degree of contact between carbide grains) and binders mean free paths d_{binder} (a measure of the thickness of the binder phase layer) were measured and calculated according to common methods, described in [10].

2.2. Indentation procedure

The indentation tests were performed using Zwick ZHU/Z2.5 apparatus. The indenters with a diameter of 3 mm were used. The indenters made from different materials were used for testing the steels and carbide composites. The steels were indented by spheres made of zirconium dioxide (ZrO_2), commercially available from Redhill. The carbide composites were tested using tungsten carbide balls (type C-2, WC, 6 wt% Co), also ordered from Redhill. The difference in the materials response related to the indenter shape is obvious if compared with indentation curves made with Berkovich indenter at nanoindentation [11], micro-macro indentations with Vickers pyramid [12], and spherical indentation, shown in Fig. 2.

The distance between indents was selected to be at least two diagonals of the indentation to avoid the influence of the first indentations on the stress distribu-
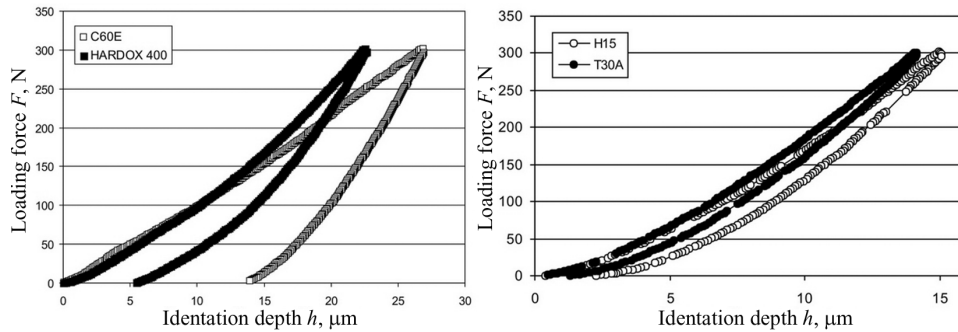
Fig. 2. Spherical indentation curves for studied materials.

tion and straining of the following indentation testing. The indentations were repeated for three times to obtain resettability of results.

The continuous measurements of the indentation depths were controlled by testing equipment Zwick ZHU/Z2.5, and then the indents residual sizes were measured using the contact type Mahr Perthometer (see Figs 3 and 4) and non-
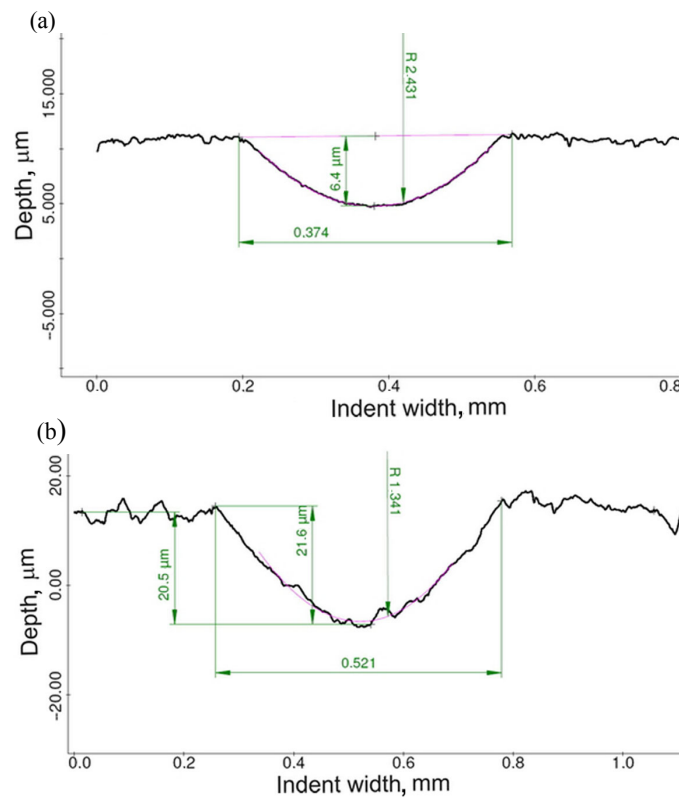

Fig. 3. Indents cross-section dimensions of HARDOX 400 (a) and C60E (b) steels for 300 N indentation load.
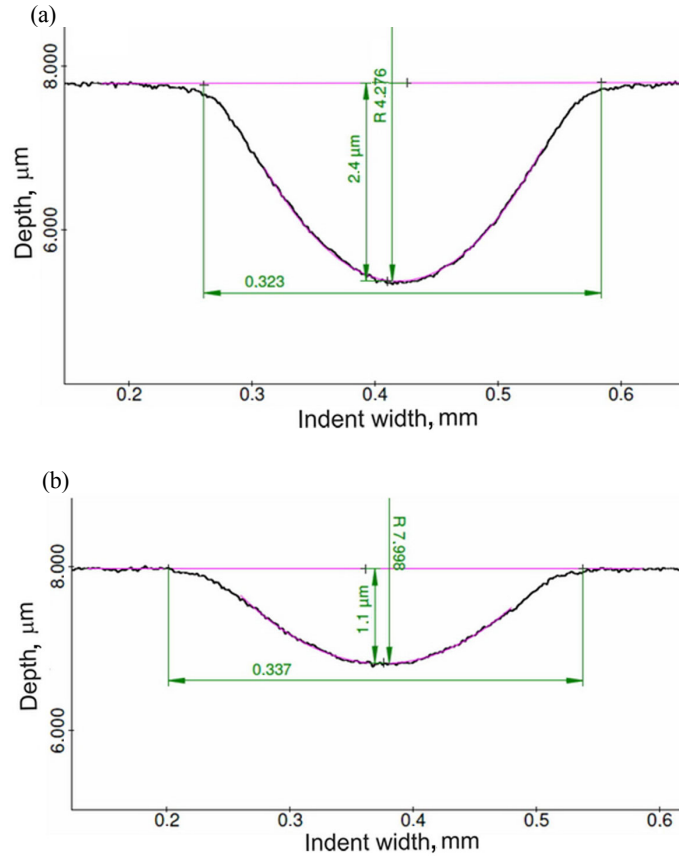
264

Fig. 4. Indents cross-section dimensions of H15 hardmetal (a) and T30A cermet (b) for 300 N indentation load.

contact 3D Optical Microscopy (Bruker ContourGT-KOX, Fig. 5). The results of the measured morphologies of the indents are illustrated with C60E steel example.

The residual radii R_r are also measured to take into account the elastic displacement of the specimen's surface, in case of carbide composites.

The residual radius shown in Fig. 5 can be used for calculation of the modified radius R^*, using equation:

$$1/R^* = 1/R - 1/R_r , \tag{1}$$

where R is the indenter radius.

The modified radius can be used for contact displacement determination from the Hertz equation:

$$h_c = a_c^2 / R^* , \tag{2}$$

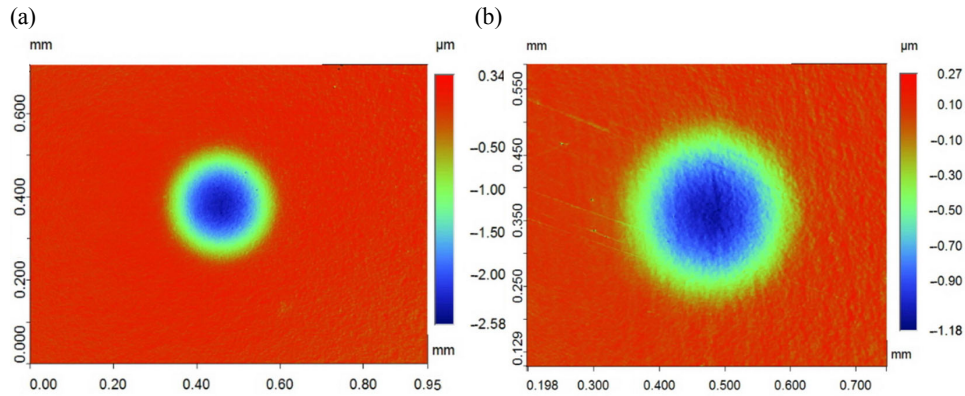where a_c is the projected contact radius.

265

Fig. 5. Indents morphologies of H15 hardmetal (a) and T30A cermet (b) for indentation load of 300 N.

The size of the projected contact area can be checked by morphology studies of the indented surfaces of the specimens. The formation of the pile-up and sink-in can be taken into consideration at that step.

Fitting of the simulation and experimental curves exclude such phenomena at all because method is dealing with load–displacement curves only.

Inverse analysis, described in [8], includes explanation how the authors avoided pile-up/sink-in measurements. The approach proposed in the current study does not need pile-up/ sink-in measurements.

3. SIMULATION PROCEDURE

For finite element analysis the program ABAQUS 6.10 was used. The numerical simulation procedure is described by several authors [13–16]. In order to prevent time-consuming investigation of the influence of different model factors on the simulation results, data from the literature was used. The inverse analysis was performed with a procedure, described by X. Chen [13].

The contact problem was modelled using axisymmetric rigid indenter as master surface interacting with axisymmetric deformable substrate as slave surface [13]. Deformed zone was meshed sufficiently fine with four-node axisymmetric elements CAX4R, similar to [14].

Concentrated force, correlated linearly with time, was chosen as a parameter under control during the simulation and was applied to the reference point of the indenter [15]. Friction was not included due to its negligible effect on the process [13]. Finally, residual stress was simulated by means of an additional load, applied on the edge of the substrate. The simulated load–displacement curves were fitted to the etalon experimental *P-h* curves by varying the type and values of the additional load, applied to the substrate or tested material in simulation.

266

4. RESULTS AND DISCUSSION

Results of the residual stress determination are shown in Table 5. Very similar results are obtained with simulation of the indentations with prescribed residual stress component in the indented material and with the inverse analysis.

Inverse analysis results revealed that implemented method heavily overestimates the yield stress $R_{p0.2}$ and residual stress σ_r values and slightly underestimates the Young's modulus. The main concern is the effect of the material strain hardening during indentation [17], which was not considered in the present study. As the maximum indentation load is sensitive to the residual stress, it is assumed to be independent of the work-hardening of the material [7].

The underestimation of the elastic modulus and overestimation of the yield stress is obviously critical for residual stress determination, and residual stress is overestimated proportionally to other overestimations. The type of stress can be estimated very precisely, compressive or tensile.

The yield stress for carbide composite is previously determined from indentation [16] and is supposed to be about 2900 MPa for H15 and 1800 MPa for T30A. Considering the difference of results, the residual stress should be at least 20 % lower for hardmetal and 50 % lower for cermet.

In future studies the deformation of the spherical indenter, indentation apparatus frame stiffness and indenter geometry imperfections should be taken into account.

5. SUMMARY

The spherical indentation can be used for the determination of the residual stress values if the work-hardening of the indented material and deformation of the spherical indenter are considered. More reliable results can be obtained for materials of plastic and plastic-elastic indentation response, like steels and Al, Cu alloys.

Comparison of experimental and FEA curves revealed that by varying the Young's modulus, plasticity data and residual stress value, it is possible to obtain almost similar load–displacement curves for tested materials, but in some cases such combination of properties conflicts with previously published data.

Table 5. Summary of obtained results

Material/Property	Elastic modulus E, GPa	Yield stress $R_{p0.2}$, MPa	Compressive residual stress σ_r, MPa
C60E	300	>410	~650
HARDOX 400	185	>1000	~780
H15	270	~4900	~3500
T30A	220	~4900	~3500

ACKNOWLEDGEMENT

REFERENCES

1. Klaasen, H. and Kübarsepp, J. Abrasive wear performance of carbide composites. *Wear*, 2006, **261**, 520–526.
2. Sergejev, F., Klaasen, H., Kübarsepp, J. and Preis, I. Fatigue mechanics of carbide composites. *Int. J. of Mater. Product Technol.*, 2011, **40**, 140–163.
3. Jang, Jae-il. Estimation of residual stress by instrumented indentation: A review. *J. Ceram. Process. Res.,* 2009, **10**, 391–400.
4. Oliver, W. C. and Pharr, G. M. An improved technique for determining hardness and elastic modulus using load and displacement sensing indentation experiments. *J. Mater. Res.*, 1992, **7**, 1564–1573.
5. Oliver, W. C. and Pharr, G. M. Measurement of hardness and elastic modulus by instrumented indentation: Advances in understanding and refinements to methodology. *J. Mater. Res.*, 2004, **19**, 3–10.
6. Ma, D., Ong, C. W. and Zhang, T. An instrumented indentation method for Young's modulus measurement with accuracy estimation. *Exp. Mech.*, 2009, **49**, 719–729.
7. Sakharova, N. A., Prates, P. A., Oliveira, M. C., Fernandes, J. V. and Antunes, J. M. A simple method for estimation of residual stresses by depth-sensing indentation. *Strain*, 2012, **48**, 75–87.
8. Chen, X., Yan, J. and Karlsson, A. M. On the determination of residual stress and mechanical properties by indentation. *Mater. Sci. Eng. A*, 2006, **416**, 139–149.
9. Chaus, A. S., Rudnitskii, F. I., Bogachik, M. and Uradnik, P. Special features of microstructure of W-Mo high-speed steel modified with titanium diboride. *Metal Sci. Heat Treatment*, 2011, **52**, 575–580.
10. Upadhyaya, G. S. *Cemented Tungsten Carbides: Production, Properties and Testing*. Noyes Publ., New Jersey, 1998.
11. Sergejev, F. Local tribo-mechanical properties of TiC-based cermets by nanoindentation. In *Proc. 14th Nordic Symposium on Tribology NORDTRIB 2010*. Storforsen, Sweden, 2010.
12. Sergejev, F., Petrov, M. and Kübarsepp, J. Determination of the mechanical properties of the carbide composites by spherical indentation. In *Proc. 8th International DAAAM Baltic Conference "INDUSTRIAL ENGINEERING"*, Tallinn, Estonia, 2012.
13. Zhao, M., Chen, X. and Yan, J. Determination of uniaxial residual stress and mechanical properties by instrumented indentation. *Acta Mater.*, 2006, **54**, 2823–2832.
14. Lee, H., Lee, J. H. and Pharr, G. M. A numerical approach to spherical indentation techniques for material property evaluation. *J. Mech. Phys. Solids*, 2005, **53**, 2037–2069.
15. Yao, Z. *Development of an Indentation Method for Material Surface Mechanical Properties Measurement.* Thesis, West Virginian University, 2005.
16. Huber, N. and Heerens, J. On the effect of a general residual stress state on indentation and hardness testing. *Acta Mater.*, 2008, **56**, 6205–6213.
17. Chiang, S. S., Marshall, D. B. and Evans, A. G. The response of solids to elastic/plastic indentation. I. Stresses and residual stresses. *J. Appl. Phys.*, 1982, **53**, 298–301.

Terastes ja karbiidkomposiitides esinevate jääkpingete hindamine kuulindentoriga koormus-sügavuskontrollitava indenteerimise teel

Fjodor Sergejev ja Mihhail Petrov

Materjalide mehaaniliste omaduste (kõvadus, purunemissitkus) hindamiseks kasutusel olevad indenteerimise ja simuleerimise meetodid on väga populaarsed oma lihtsuse tõttu. Selleks ei ole vajalik keerulise kuju ja suure geomeetrilise täpsusega katsekehade ettevalmistamine, saab kasutada standardseid seadmeid, palju mõõtmisi saab teostada väiksemõõtmelistel katsekehadel. Viimased uurimised on tõestanud võimalust materjalide jääkpingete määramiseks kombineeritud indenteerimise-simuleerimise katsete abil.

Käesolev uurimus on esimene katse hinnata karbiidkomposiitides (kõvasulam ja kermis) tekkivate jääkpingete suurust ning tüüpi, kasutades kombineeritud katsetusviisi. Katsetati mitmeid laialt kasutatavaid teraseid.

Jääkpingete hindamiseks on esitatud täiustatud kuulindentoriga indenteerimise simuleerimise algoritm. Simuleerimise tulemusi on võrreldud katsetulemustega.